

pubs.acs.org/JPCA Article

Role of Explicit Hydration in Predicting the Aqueous Standard Reduction Potential of Sulfate Radical Anion by DFT and Insight into the Influence of pH on the Reduction Potential

Asa E. Carre-Burritt, Daniel J. Van Hoomissen, and Shubham Vyas*



Cite This: J. Phys. Chem. A 2022, 126, 1422–1428



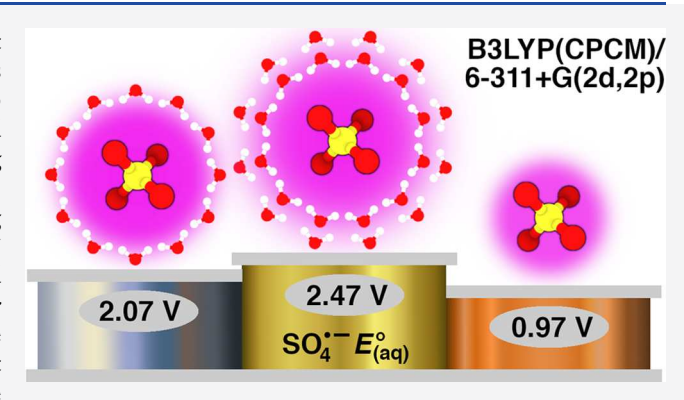
ACCESS I

Metrics & More

Article Recommendations

s Supporting Information

ABSTRACT: Sulfate radical anion $(SO_4^{\bullet-})$ is a potent oxidant capable of destroying recalcitrant environmental contaminants such as perfluoroalkyl carboxylic acids. In addition, it is thought to participate in important atmospheric reactions. Its standard reduction potential (E°) is fundamental to its reactivity. Using theoretical methods to accurately predict the aqueous phase E° requires solvation with explicit water molecules. Herein, using density functional theory, we calculated the aqueous E° of $SO_4^{\bullet-}$ and evaluated sensitivity to explicit water count. The E° increased considerably with more waters until ca. 24 were included, after which change in E° was small. When a proton was added to these systems, the E° was similar regardless of the explicit water count and this value was similar to the E° for systems with a large



number of explicit waters but no proton. This result agrees with literature evidence that the E° is pH independent. Natural Bond Orbital natural population analysis indicated that in the case of both SO_4^{2-} and $SO_4^{\bullet-}$, considerable charge was donated from the SO_4 center to the explicit solvation shells.

■ INTRODUCTION

Activating persulfate $(S_2O_8^{2-})$ to produce sulfate radical anion $(SO_4^{\bullet-})$ is a noteworthy approach to destroying recalcitrant environmental contaminants in water. $^{1-3}$ $SO_4^{\bullet-}$ is a potent oxidant that can destroy contaminants in situations where other advanced oxidation processes (AOPs) (e.g., the Fenton reaction) might be insufficient such as is the case of perfluoroalkyl carboxylic acid (PFCA) mineralization. $^{4-6}$ $SO_4^{\bullet-}$ is also an important species in atmospheric chemistry that had been theorized to participate in SO_2 oxidation leading to H_2SO_4 formation. Furthermore, its potential role in atmospheric pollutant transformations has also been considered.

SO₄• is selective for single electron transfer (SET) although it can also perform hydrogen atom abstraction and addition to double bonds. ^{1,10,11} The thermodynamic favorableness of electron transfer (ET) is provided by comparing the standard reduction potentials (*E*°s) of the electron donor and the electron acceptor. ^{12,13} In fact, the difference in reduction potentials between reactants is the thermodynamic driving force of ET. This parameter, coupled with the reorganization energy required for ET, determines the ET activation energy. ¹³ Previously, researchers have used electronic and free energy values from density functional theory (DFT) studies in order to determine ET transition state energies and predict ET kinetics for reactions between SO₄• and environmental

contaminants. 14,15 These studies did not individually report the E° s for the electrochemical half-reactions that were involved. We put forth that these values are useful benchmarks for evaluating the accuracy of the computational model being employed.

The prior literature employed dielectric continuum (implicit) solvation models to account for the aqueous reaction environment. However, implicit solvation becomes inaccurate for systems with regions of highly concentrated charge. 12 SO₄ $^{2-}$, the product of SET from a substrate to SO₄ $^{\bullet-}$, exemplifies such a scenario, being a highly kosmotropic ion that interacts strongly with it is solvation shell. For such a system, it is appropriate to explicitly include solvent molecules. Herein, we report the first estimations of the E° of SO₄ $^{\bullet-}$ as a function of explicit water numbers and these calculations are benchmarked against the empirical value, 2.437 V vs SHE.

In addition to including explicit water molecules in our calculations, we explored systems that also included a proton. Within the literature, there are reports of enhanced PFCA

Received: November 1, 2021 Revised: January 14, 2022 Published: February 16, 2022





degradation by thermally activated persulfate at low pH. ¹⁸ One theory to explain this phenomenon is that sulfate radical protonation occurs, leading to a higher E° for putative HSO_4^{\bullet} vs $SO_4^{\bullet-}$ as well as reduced electrostatic repulsion between the PFCA and the radical oxidant. ^{15,18} Nonetheless, to the best of our knowledge, there is no literature report of an increased E° for $SO_4^{\bullet-}$ at low pH. Our proton-bearing systems provide insight into the effect of pH on the E° of $SO_4^{\bullet-}$.

■ COMPUTATIONAL DETAILS

Computational work was performed using the Gaussian 09(d.01) software suite. ¹⁹ The initial molecular coordinates used to discover stationary points for $[SO_4(H_2O)_n]^{2-}$ were gas-phase low-energy structures from Kulichenko et al., who optimized initial coordinates taken from prior art (vide infra), except in the n = 3 case, for which the structure was a putative potential energy global minimum (GM) structure obtained using the Coalescence Kick procedure. ²⁰ For n = 6, the original structure was a putative GM structure taken from Wang et al., which was determined by comparing electron binding energies of structures evaluated by ab initio methods with photoelectron spectra of hydrated sulfate clusters.²¹ For n = 9-40, the original structures were taken from Smeeton et al., who represented SO₄²⁻ and water molecules as rigid bodies and applied force fields in a basin-hopping algorithm to find lowenergy isomers.²² This approach reproduced previously reported GM structures for $n \le 6$ as low-energy isomers or as global minima.

In this study, structures from Kulichenko et al. were submitted to geometry optimization at a given level of theory, and the presence of a stationary point for each structure reported herein was confirmed by analytical frequency calculations. The resulting coordinates were taken as the starting points to discover stationary points for $[SO_4(H_2O)_n]^{\bullet-}$ for which geometry optimizations were performed using a charge and multiplicity of -1 and 2. The starting structures for $H^{+}[SO_4(H_2O)_n]^{2-}$ were obtained by taking the initial molecular coordinates for $[SO_4(H_2O)_n]^{2-}$ and incorporating a proton coordinated to either the SO₄ center or one of the water molecules within the first solvation shell, while slightly adjusting the orientation of the water molecules along a corresponding hydrogen bond network to account for the additional proton. Stationary points for $H^+[SO_4(H_2O)_n]^{\bullet-}$ were then obtained according to a protocol analogous to that for $[SO_4(H_2O)_n]^{2-}$ and $[SO_4(H_2O)_n]^{\bullet-}$ as described above. Additional $[SO_4(H_2O)_n]^{2-}$ isomers reported in Figure S3 were obtained by arranging explicit water molecules in distinct hydrogen bonding networks around the SO₄ center. Corresponding $[SO_4(H_2O)_n]^{\bullet-}$ isomers were then obtained by oxidizing and reoptimizing the resulting stationary point structures.

Natural atomic population analysis was performed using the NBO program, ²³ and NBO spin was calculated by taking the difference between α and β natural populations.

RESULTS AND DISCUSSION

Standard Reduction Potential Calculations. The aqueous phase E° of $SO_4^{\bullet-}$ was calculated according to eq 1 at the B3LYP(CPCM)/6-311+G(2d,2p) level of theory from systems using 0, 3, 6, 9, 12, 18, 24, 27, 30, and 40 explicit water molecules in the solvation shells of $SO_4^{\bullet-}$ and SO_4^{2-} (Figure 1). ΔG_{rxn} corresponds to eq 2, F is the Faraday constant and

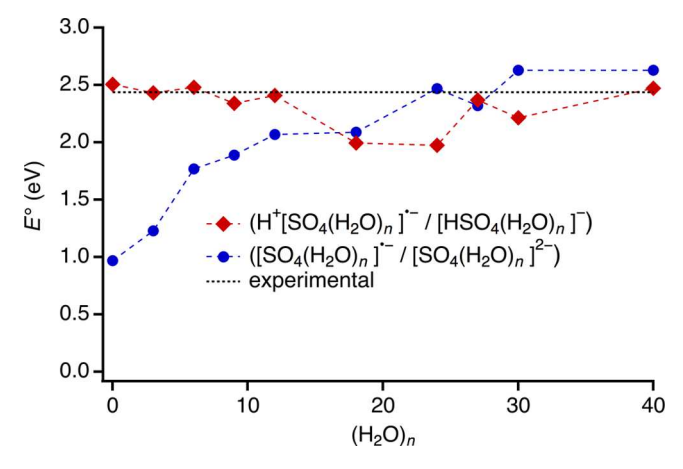


Figure 1. $SO_4^{\bullet-}E^{\circ}$ for systems with increasingly greater numbers of explicit water molecules (blue trace) and then for similar systems that included a proton (red trace). The empirical E° is the horizontal dashed line. Proton-bearing radical systems involved HSO_4^{\bullet} and $[HSO_4(H_2O)_3]^{\bullet}$ for 0 and 3 explicit water molecules and $H_3O^+[SO_4(H_2O)_{n-1}]^{\bullet-}$ CIPs or SBIPs for 6–40 explicit waters. Proton-bearing reduced systems consisted of $[HSO_4(H_2O)_n]^-$. Calculations were performed at the B3LYP(CPCM)/6-311+G-(2d,2p) level of theory.

 $E_{\rm SHE}=4.47~{\rm V}$, an empirical value. ¹² For 0 explicit water molecules, the E° begins at 0.97, which is far below the experimental value of 2.437 V, ¹⁷ demonstrating that implicit solvation is inadequate for estimating the thermodynamic properties of this system. With an increasing number of explicit waters, E° values increased considerably at first until the region of 24–40 explicit waters, within which additional waters provided minimal change in E° values and within this region E° s were near the empirical value. Similar results were obtained using the IEF-PCM and SMD implicit solvent models (Figure S1). M06-2X and ω B97-XD functionals were also investigated, and these functionals substantially overestimated the E° when large numbers of explicit waters were used but demonstrated similar trends with respect to the response of E° to explicit water molecule count (Figure S2). The remainder of results discussed were obtained using B3LYP(CPCM).

To probe whether the observed trend in E° as a function of explicit water count was an artifact of insufficient conformation space sampling, isomers with different arrangements of waters around the SO_4 center were investigated for both singlet and radical systems with 3–18 explicit waters. A similar trend was observed as to when only the low-energy arrangements from Kulichenko et al. were used as starting geometries (Figure S3).

$$E^{\circ} = \frac{-\Delta G_{\text{rxn}}}{F} - E_{\text{SHE}} \tag{1}$$

$$SO_4^{\bullet -} + e^- \rightarrow SO_4^{2-} \tag{2}$$

The Empirical Benchmark. At first it seemed difficult to benchmark our calculations because aqueous phase reduction potentials quoted in the literature vary considerably. For example, a range of 2.52–3.08 V vs NHE is commonly referenced. However, the upper value in this range was derived from efforts to fit Marcus theory electron transfer kinetic parameters to experimental rate constants for the reactions between ArH and $SO_4^{\bullet-24}$ and it lacks a direct empirical basis. The lower value in this range was determined from tabulated thermodynamic values. Ultimately, various

approaches have been taken to estimate the aqueous E° of $SO_4^{\bullet-.17,26}$ We favor the value of 2.437 \pm 0.019 vs SHE determined using an active thermochemical tables method, which was provided in an IUPAC technical report.¹⁷

Reduction Potential Estimations from Computed Electrochemical Cell Potentials. We investigated whether it was possible to exclude explicit water molecules and account for solvation error by referencing the $SO_4^{\bullet-}$ E° against halfreactions calculated at the same level of theory (Table 1).

Table 1. $SO_4^{\bullet-}E^{\circ}$ Values Estimated Using a Reference Half-Reaction^a

electrochemical cell	$egin{aligned} E_{ m cell} \ ({ m V}) \end{aligned}$	$\underset{C_{\mathrm{cell}}}{\operatorname{literature}} V)$	estimated $SO_4^{\bullet-}$ E° (V)
$SO_4^{\bullet -} + CO_3^{2-}$ $\rightarrow SO_4^{2-} + CO_3^{\bullet -}$	+1.33	+0.87	+2.90
$SO_4^{\bullet-} + Cl^- \rightarrow SO_4^{2-} + Cl^{\bullet}$	-1.25	+0.01	+1.18
$SO_4^{\bullet -} + SCN^-$ $\rightarrow SO_4^{2-} + SCN^{\bullet}$	-0.37	+0.83	+1.24

"Calculations were performed at the B3LYP(CPCM)/6-311+G-(2d,2p) level of theory.

Three different reference redox couples were investigated: (SCN^{\bullet}/SCN^{-}) , (Cl^{\bullet}/Cl^{-}) , and $(CO_{3}^{\bullet-}/CO_{3}^{2-})$. The last couple in this series bears the same charge as the $(SO_{4}^{\bullet-}/SO_{4}^{2-})$ couple, and CO_{3}^{2-} is a highly kosmotropic ion like SO_{4}^{2-} . The 2.90 V $SO_{4}^{\bullet-}$ E° estimated using this reference couple was closer to the benchmark value than when the other reference couples were used, but it was still further away than the value obtained by using a large number of explicit water molecules and referencing against the empirical SHE potential.

Proton-Bearing Redox Couples. In order to gain insight to the influence pH has on the electron transfer behavior of $SO_4^{\bullet-}$, we added a proton into our systems. For the reduced proton-bearing systems $(H^+[SO_4(H_2O)_n]^{2-})$ consisting of 0–40 explicit waters, stationary points were found consisting of an HSO_4 center $([HSO_4(H_2O)_n]^-)$. In addition, contact ion pairs

(CIPs) were found for 9–40 explicit waters, and solvent-bridged ion pairs (SBIPs) were found for 12–40 explicit waters. Ion pairs will be denoted as $H_3O^+[SO_4(H_2O)_{n-1}]^{2-}$. Ion pairs were not found for lower numbers of explicit waters because those optimizations exclusively yielded $[HSO_4(H_2O)_n]^-$.

Within the radical proton-bearing systems $(H^{+}[SO_{4}(H_{2}O)_{n}]^{\bullet-})$, the only case that HSO_{4}^{\bullet} was observed was in the absence of explicit water molecules or when only three were included as shown in Figure 2. With six or more explicit waters, the proton was coordinated to a water molecule within the solvation shell of $SO_4^{\bullet-}$ to form an ion pair $(H_3O^+[SO_4(H_2O)_{n-1}]^{\bullet-})$. A three explicit water ion pair was also found. In a previous study, we found that there was no stationary point corresponding to ${\rm HSO_4}^{\bullet}$ in the presence of three and six water molecules. ²⁸ In that study, ${\rm H_3O^+}$ was coordinated by two H2O molecules, whereas in the present study the three explicit H₂O molecules were spatially separated from each other. Beyond the structures already described, there were no other isomers involving HSO_4^{\bullet} found at any level theory we investigated, excluding incorrect structures within which the solvation shell was oxidized and anticipated HSO₄• was actually HSO₄-.

In the radical systems, the stereoelectronics of the SO_4 center shared many similarities (Table S1). In the absence of explicit water molecules, $SO_4^{\bullet-}$ had approximately $C_{2\nu}$ symmetry, while HSO_4^{\bullet} sans explicit waters had reduced symmetry that was approximately C_s . For $SO_4^{\bullet-}$, the NBO spin on two of the four $SO_4^{\bullet-}$ oxygen atoms was 0.98 au (with 0.49 au at each oxygen) which is close to the total NBO spin of 1 au; meanwhile, considerably more negative charge was present on the other two oxygen atoms. The results are in good agreement with prior theoretical work. ^{29,30} The structures with explicit waters with or without a proton were in close approximation to the aforementioned stereoelectronic characteristics (Figure 2). The NBO spin on two of the four SO_4

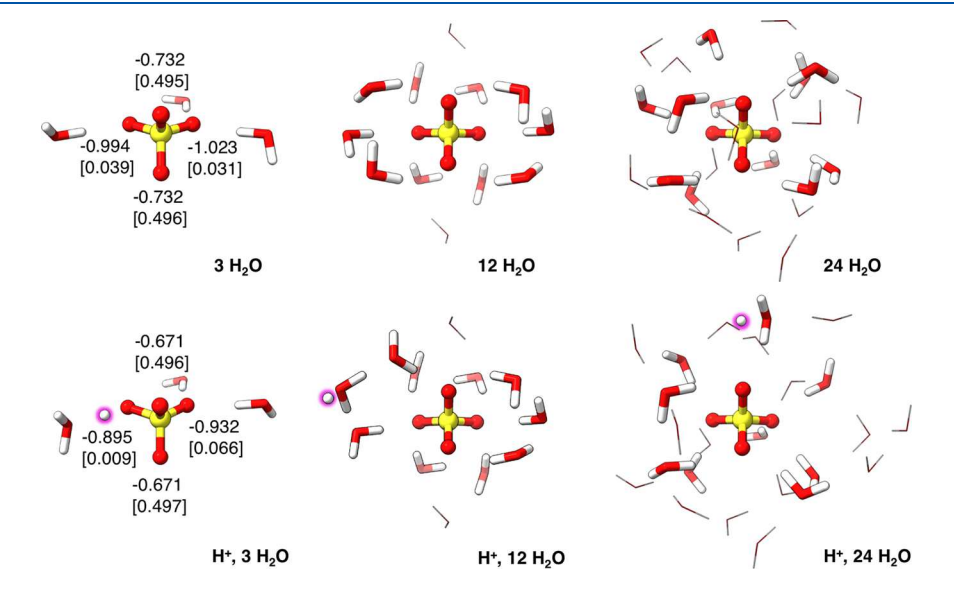


Figure 2. (Top) Examples of $SO_4^{\bullet-}$ structures of with 3, 12, and 24 explicit water molecules. (Bottom) Similar structures that include a proton (which is highlighted in fuchsia). For three explicit waters, the stationary point involves $HSO_4^{\bullet-}$. For all structures, waters in the first solvation shell of $SO_4^{\bullet-}$ are shown as sticks, and those in the second shell are shown as lines. Structures with three explicit waters include the natural charge (au) on each SO_4 oxygen and the corresponding NBO spin (au) in brackets. Geometry optimizations were performed at the B3LYP(CPCM)/6-311+G(2d,2p) level of theory.

oxygens for $[SO_4(H_2O)_n]^{\bullet-}$ and $H^+[SO_4(H_2O)_n]^{\bullet-}$ for all n was 0.991 \pm 0.006 au (1σ) .

In stark contrast to the systems without a proton, when no explicit water molecules were included, the calculated E° was 2.51 V (Figure 1). Interestingly, adding explicit water molecules did not substantially alter this value. E° values for systems including a proton and any number of explicit waters were similar to E° values for systems without a proton and large numbers of explicit waters. The calculated E° s were relatively insensitive to the position of the proton and similar E° s were calculated when the redox couple involved (HSO₄ $^{\bullet}$ / HSO_4^-), $(H_3O^+SO_4^{\bullet-}/HSO_4^-)$, or $(H_3O^+SO_4^{\bullet-}/H_3O^+SO_4^{2-})$, with an average value of 2.29 \pm 0.17 V (1σ) . For example, the ($[HSO_4(H_2O)_3]^{\bullet}/[HSO_4(H_2O)_3]^{-}$) redox couple had a 2.43 V E° , while the $(H_3O^+[SO_4(H_2O)_2]^{\bullet-}/$ $[HSO_4(H_2O)_3]^-$) couple had a 2.24 V E° ; both were within 1σ of the average value for proton-bearing redox couples. Meanwhile, $(H_3O^+[SO_4(H_2O)_{n-1}]^{\bullet-}/H_3O^+[SO_4(H_2O)_{n-1}]^{2-}$ CIP or SBIP) redox couples had very similar E°s to $\left(H_3O^+[SO_4(H_2O)_{n-1}]^{\bullet-}/[HSO_4(H_2O)_n]^-\right) \ \ redox \ \ couples$ (Figure S4).

The similar E° s for systems with or without a proton (as long as sufficient explicit water molecules were included in systems without a proton) is in accord with the chemical literature in which no pH dependence for the E° of $SO_4^{\bullet-}$ has been described to the best of the authors' knowledge. Furthermore, one can estimate the E° of $SO_4^{\bullet-}$ under acidic conditions using the equilibrium present in eq 3. This equilibrium is equal to the ratio between the corresponding forward and reverse reaction rates ($k_{forward} = 3.5 \pm 0.5 \times 10^5 \, \mathrm{M}^{-1} \, \mathrm{s}^{-1}$, $k_{reverse} = 6.49 \, \mathrm{M}^{-1} \, \mathrm{s}^{-1}$ using the molarity of water = 55.5 M^{31}).

$$OH^{\bullet} + HSO_{4}^{-} \underset{k_{rowrse}}{\overset{k_{forward}}{\rightleftharpoons}} H_{2}O + SO_{4}^{\bullet -}$$
(3)

Application of eq 4 to chemical eq 3 provides a 27 kJ mol⁻¹ better stability of the products vs reactants, corresponding to a 0.28 V difference in potential for 1 e⁻ transfer. Referencing this difference to the known E° for the (H⁺, OH[•]/H₂O) redox couple, 2.73 V, provides a E° for the (H⁺, SO₄•-/HSO₄-) redox couple of 2.45 V. This value is within error of the value for the (SO₄•-/SO₄²⁻) redox couple: 2.437 \pm 0.019 V.¹⁷ This suggests that the E° of SO₄•- is largely insensitive to pH.

$$K = \exp\left(\frac{-\Delta G_{equilib}}{RT}\right) \tag{4}$$

Linear Correlation Between Frontier Molecular Orbital Energies and Standard Reduction Potentials. The reduction potential for a given species is often linearly correlated to its HOMO or SOMO/LUMO energy (depending on whether the reduced or oxidized species in the redox couple is being considered). The E° values for $([SO_4(H_2O)_n]^{\bullet-}/[SO_4(H_2O)_n]^{2-})$ redox couples reported herein were linearly correlated to $[SO_4(H_2O)_n]^{2-}$ HOMO energy levels with an R^2 value of 0.933 (Figure 3). The HOMO-1 energies were nearly degenerate and showed a similar linear correlation (HOMO and HOMO-1 isosurfaces are shown in Figure S8). In addition, β electron $[SO_4(H_2O)_n]^{\bullet-}$ LUMO energy levels were linearly correlated to the corresponding E° s with a 0.963 R^2 . However, for proton-bearing systems there was little linear correlation between E° s and frontier molecular orbital

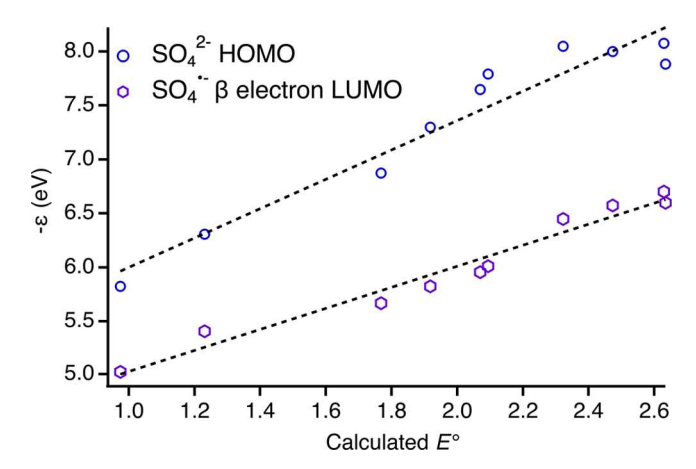


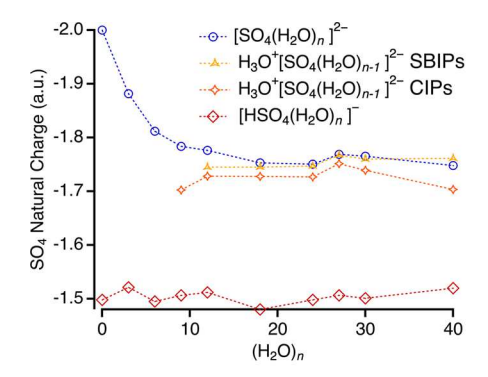
Figure 3. Linear relationship between calculated E° s for $([SO_4(H_2O)_n]^{\bullet-}/[SO_4(H_2O)_n]^{2-})$ redox couples and $[SO_4(H_2O)_n]^{2-}$ HOMO energies or $[SO_4(H_2O)_n]^{\bullet-}$ β electron LUMO energies.

energies, with R^2 values less than or equal to 0.34 (Figures S5 and S6).

Charge Transfer To Solvent. It is evident in Figure 1 that in the chemical computations, the interaction of $SO_4^{\bullet-}$ and/or SO_4^{2-} with their solvent shells contributes dramatically to calculated E° s. It is well-known that SO_4^{2-} is stabilized by water molecules, requiring at least three to stabilize the Coulomb repulsion preventing the isolation of $SO_4^{2-20,33,34}$ Furthermore, SO_4^{2-} has a large, SO_4^{2-} kJ mol⁻¹, enthalpy of hydration. We investigated the stabilization of SO_4^{2-} as well as $SO_4^{\bullet-}$ as a function of explicit water count by characterizing the charge localized on SO_4 and SO_4 centers by Natural Bond Orbital (NBO) natural population analysis. Both systems with and without a proton were explored. Results of this analysis are presented in Figure 4.

In systems without a proton, the natural charge on SO_4^{2-} decreased considerably with the addition of a few explicit water molecules. As the number of explicit waters increased, the decrease in natural charge on the SO₄ center was continually less on a per-water basis. Overall, there was a decrease in natural charge on SO₄ from -2.00 to -1.75 au between 0 and 40 explicit water molecules, in good agreement with the results of Kulichenko et al.²⁰ It is important to note that even when no explicit waters were included, the CPCM implicit solvent model was employed, and the natural charge on the SO₄ center was -2.00 au. This highlights the inadequacy of implicit solvation models—which do not properly treat charge transfer to solvent 36,37 —to characterize the stabilization of SO_4^{2-} by its aqueous environment. For SO4 on the SO4 center decreased from -1.00 to -0.92 au between 0 and 40 explicit water molecules. Evidently, $SO_4^{\bullet-}$ can also be stabilized through interactions with its solvation shell. Presumably, convergence of charge transfer with respect to explicit water count indicates that a sufficiently large solvent shell has been incorporated.

The charge distribution in the systems incorporating a proton is more intricate. When the proton was coordinated to SO_4^{2-} to form HSO_4^{-} , the natural charge on the SO_4 center was consistently near -1.50 au regardless of explicit water count. Meanwhile, taking into consideration the proton, the natural charge localized on the HSO_4 center remained near -1.0 au, deviating a maximum of 0.05 au. Of course, one must also consider the contribution of electron density from water



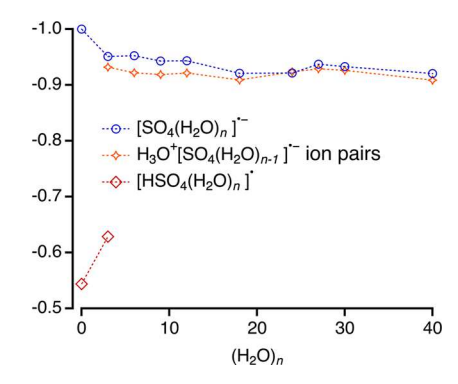


Figure 4. Natural charge on SO_4 centers for SO_4^{2-} and $SO_4^{\bullet-}$ ions in water clusters with or without a proton as a function of explicit water count. Radical systems ion pairs are either CIPs or SBIPs.

molecules coordinated to this acidic proton when explicit waters are included, yet we reiterate that the natural charge on the SO_4 center remained similar. Ultimately, these results demonstrate that HSO_4^- contributes considerably less charge to its solvation shell than $SO_4^{\ 2^-}$, and is consistent the empirical observation that HSO_4^- alone in the gas phase has a positive vertical electron detachment energy. In the stationary points consisting of CIPs and SBIPs, the natural charge on the SO_4 center did not dramatically change with explicit water count either. The natural charge on the SO_4 center in SBIP systems was similar to systems that excluded a proton but that had a large number of explicit waters. In CIP systems, the natural charge on the SO_4 center was smaller than in SBIP systems but of similar magnitude.

The natural charge analysis for radical systems that included a proton was also interesting. The zero and three explicit water structures involved ${\rm HSO_4}^{\bullet}$, and there was much less natural charge on the ${\rm SO_4}$ center as compared to the structures with greater numbers of explicit waters wherein the proton was coordinated instead to water. For ${\rm H_3O^+}$ ion-paired ${\rm SO_4}^{\bullet-}$, the natural charge on the ${\rm SO_4}$ center was consistently near -0.92 au: the value to which the ${\rm SO_4}$ natural charged seemed to converge with increasing explicit waters in systems without a proton. Evidently, having ${\rm H_3O^+}$ proximal to the ${\rm SO_4}$ center affected its natural charge similarly to incorporating a large number of explicit waters.

CONCLUSION

Our DFT results demonstrated that $SO_4^{\bullet-}$ and SO_4^{2-} both interact with explicit aqueous solvent shells through charge transfer, and furthermore that explicit solvation dramatically influenced the E° calculated for their redox couple relative to only using an implicit continuum solvent model. Furthermore, when a proton was added to these systems, it was seen that the E° changed minimally as a function of explicit water count, at least for the specific structures and corresponding redox couples reported herein. Notably, in these cases, there was little change in charge of the SO₄ center. These results suggest that charge transfer to solvent is descriptive of the role explicit solvation plays in modulating calculated E° values. Interestingly, there was a strong linear correlation between both the $[SO_4(H_2O)_n]^{2-}$ HOMO and $[SO_4(H_2O)_n]^{\bullet-}$ β electron LUMO energies and the corresponding E° that was calculated, whereas for proton-bearing systems there was little linear correlation.

Our characterization of the impact explicit solvation has on $(SO_4^{\bullet -}/SO_4^{2-})$ redox couple properties will greatly accelerate

efforts to model electron transfer kinetics for reactions involving $SO_4^{\bullet-}$ in the aqueous phase. The different physicochemical properties of $SO_4^{\bullet-}$ that we describe for different sized $SO_4^{\bullet-}(H_2O)_n$ water clusters will also provide useful insight to researchers investigating the atmospheric reactions of $SO_4^{\bullet-}$ considering that hydration is an important aspect of that chemistry. S,38

Further work is needed to determine which DFT functionals are most appropriate for quantitatively evaluating the E° of $\mathrm{SO_4}^{\bullet-}$. In addition, it remains to be understood why the $(\mathrm{SO_4}^{\bullet-}, \mathrm{H^+/HSO_4}^-)$ redox couple has the same E° value as the redox couples without a proton when sufficient explicit water molecules are included. Finally, the extent to which incorporating a representative population of solvent shell conformations influences E° calculations remains to be determined, and this is a known challenge for the explicit/implicit solvation approach used herein. 12

ASSOCIATED CONTENT

Supporting Information

The Supporting Information is available free of charge at https://pubs.acs.org/doi/10.1021/acs.jpca.1c09459.

Reduction potentials calculated using other implicit solvent models and additional density functionals, calculated reduction potentials considering additional explicit water arrangements, frontier MO and reduction potential relationships for proton-bearing systems, radical system geometrical parameters, reduced system MO isosurfaces, and stationary point molecular coordinates (PDF)

AUTHOR INFORMATION

Corresponding Author

Shubham Vyas — Department of Chemistry, Colorado School of Mines, Golden, Colorado 80401, United States;
orcid.org/0000-0002-5849-8919; Phone: 303-273-3632; Email: svyas@mines.edu

Authors

Asa E. Carre-Burritt — Department of Chemistry, Colorado School of Mines, Golden, Colorado 80401, United States Daniel J. Van Hoomissen — Department of Chemistry, Colorado School of Mines, Golden, Colorado 80401, United States

Complete contact information is available at: https://pubs.acs.org/10.1021/acs.jpca.1c09459

Notes

The authors declare no competing financial interest.

ACKNOWLEDGMENTS

This work was funded by the National Science Foundation (CHE-1710079). The authors also acknowledge the computational resources allocated by the high-performance computing facility at the Colorado School of Mines.

REFERENCES

- (1) Wojnárovits, L.; Takács, E. Rate constants of sulfate radical anion reactions with organic molecules: A review. *Chemosphere* **2019**, 220, 1014–1032.
- (2) Hori, H.; Yamamoto, A.; Hayakawa, E.; Taniyasu, S.; Yamashita, N.; Kutsuna, S.; Kiatagawa, H.; Arakawa, R. Efficient Decomposition of Environmentally Persistent Perfluorocarboxylic Acids by Use of Persulfate as a Photochemical Oxidant. *Environ. Sci. Technol.* **2005**, 39, 2383–2388.
- (3) Hori, H.; Nagaoka, Y.; Murayama, M.; Kutsuna, S. Efficient Decomposition of Perfluorocarboxylic Acids and Alternative Fluorochemical Surfactants in Hot Water. *Environ. Sci. Technol.* **2008**, 42, 7438–7443.
- (4) Javed, H.; Lyu, C.; Sun, R.; Zhang, D.; Alvarez, P. J. Discerning the inefficacy of hydroxyl radicals during perfluorooctanoic acid degradation. *Chemosphere* **2020**, 247, 125883.
- (5) Tang, H.; Xiang, Q.; Lei, M.; Yan, J.; Zhu, L.; Zou, J. Efficient degradation of perfluorooctanoic acid by UV-Fenton process. *Chemical Engineering Journal* **2012**, *184*, 156–162.
- (6) Trojanowicz, M.; Bojanowska-Czajka, A.; Bartosiewicz, I.; Kulisa, K. Advanced Oxidation/Reduction Processes treatment for aqueous perfluorooctanoate (PFOA) and perfluorooctanesulfonate (PFOS) A review of recent advances. *Chemical Engineering Journal* **2018**, 336, 170–199.
- (7) Finlayson-Pitts, B. J.; Pitts, J. N. In *Chemistry of the Upper and Lower Atmosphere*; Finlayson-Pitts, B. J., Pitts, J., Eds.; Academic Press: San Diego, CA, 2000; Chapter 8, pp 294–348.
- (8) Tsona, N. T.; Bork, N.; Vehkamäki, H. Exploring the chemical fate of the sulfate radical anion by reaction with sulfur dioxide in the gas phase. *Atmospheric Chemistry and Physics* **2015**, *15*, 495–503.
- (9) Kutsuna, S.; Koike, K.; Hori, H. Rate Constants and Conversion Ration for Aqueous-Phase Reactions of SO4.- with CnF2n+1C(O)O-(n = 4-7) at 298 K. *International Journal of Chemical Kinetics* **2009**, 41, 735-747.
- (10) Neta, P.; Madhavan, V.; Zemel, H.; Fessenden, R. W. Rate Constants and Mechanism of Reaction of SO₄• with Aromatic Compounds. *J. Am. Chem. Soc.* **1977**, *99*, 163–164.
- (11) Khursan, S. L.; Semes'ko, D. G.; Teregulova, A. N.; Safiullin, R. L. Analysis of the Reactivities of Organic Compounds in Hydrogen Atom Abstraction from Their C-H bonds by the Sulfate Radical Anion SO₄•-. *Kinetics and Catalysis* **2008**, 49, 202–211.
- (12) Ho, J.; Coote, M. L.; Cramer, C. J.; Truhlar, D. G. In *Organic Electrochemistry*, 5th ed.; Hammerich, O., Speiser, B., Eds.; CRC Press: Boca Raton, FL, 2015; Chapter 4, pp 229–260.
- (13) Piechota, E. J.; Meyer, G. J. Introduction to Electron Transfer: Theoretical Foundations and Pedagogical Examples. *J. Chem. Educ.* **2019**, *96*, 2450–2466.
- (14) Luo, S.; Wei, Z.; Dionysiou, D. D.; Spinney, R.; Hu, W. P.; Chai, L.; Yang, Z.; Ye, T.; Xiao, R. Mechanistic insight into reactivity of sulfate radical with aromatic contaminants through single-electron transfer pathway. *Chemical Engineering Journal* **2017**, 327, 1056–1065.
- (15) Zhang, Y.; Moores, A.; Liu, J.; Ghoshal, S. New Insights into the Degradation Mechanism of Perfluorooctanoic Acid by Persulfate from Density Functional Theory and Experimental Data. *Environ. Sci. Technol.* **2019**, *53*, 8672–8681.
- (16) O'Brien, J. T.; Prell, J. S.; Bush, M. F.; Williams, E. R. Sulfate Ion Patterns Water at Long Distance. J. Am. Chem. Soc. 2010, 132, 8248–8249.

- (17) Armstrong, D. A.; Huie, R. E.; Koppenol, W. H.; Lymar, S. V.; Merenyi, G.; Neta, P.; Ruscic, B.; Stanbury, D. M.; Steenken, S.; Wardman, P. Standard electrode potentials involving radicals in aqueous solution: Inorganic radicals (IUPAC Technical Report). *Pure Appl. Chem.* **2015**, *87*, 1139–1150.
- (18) Bruton, T. A.; Sedlak, D. L. Treatment of perfluoroalkyl acids by heat-activated persulfate under conditions representative of in situ chemical oxidation. *Chemosphere* **2018**, *206*, 457–464.
- (19) Frisch, M. J.; Trucks, G. W.; Schlegel, H. B.; Scuseria, G. E.; Robb, M. A.; Cheeseman, J. R.; Scalmani, G.; Barone, V.; Mennucci, B.; Petersson, G. A. et al. *Gaussian 09*, Rev. D.01; Gaussian Inc.: Wallingford, CT, 2009.
- (20) Kulichenko, M.; Fedik, N.; Bozhenko, K. V.; Boldyrev, A. I. Hydrated Sulfate Clusters SO_4^{2-} (H_2O)_n (n=1-40): Charge Distribution Through Solvation Shells and Stabilization. *J. Phys. Chem. B* **2019**, *123*, 4065–4069.
- (21) Wang, X.-B.; Sergeeva, A. P.; Yang, J.; Xing, X.-P.; Boldyrev, A. I.; Wang, L.-S. Photoelectron Spectroscopy of Cold Hydrated Sulfate Clusters, SO4 2-(H2O)n (n) 4–7): Temperature-Dependent Isomer Populations. *J. Phys. Chem. A* **2009**, *113*, 5567–5576.
- (22) Smeeton, L. C.; Farrell, J. D.; Oakley, M. T.; Wales, D. J.; Johnston, R. L. Structures and Energy Landscapes of Hydrated Sulfate Clusters. *J. Chem. Theory Comput.* **2015**, *11*, 2377–2384.
- (23) Glendening, E. D.; Reed, A. E.; Carpenter, J. E.; Weinhold, F. NBO, Ver. 3.1.
- (24) Eberson, L. Reactivity and Structure: Concepts in Organic Chemistry, 1st ed.; Springer-Verlag: Berlin and Heidelberg, Germany, 1987; Vol. 25.
- (25) Neta, P.; Huie, R. E.; Ross, A. B. Rate Constants for Reactions of Inorganic Radicals in Aqueous Solution. *J. Phys. Chem. Ref. Data* 1988, 17, 1027–1284.
- (26) Stanbury, D. M. Reduction Potentials Involving Inorganic Free Radicals in Aqueous Solution. *Adv. Inorg. Chem.* **1989**, *33*, 69–138.
- (27) Zhang, Y.; Cremer, P. S. Interactions between macromolecules and ions: the Hofmeister series. *Curr. Opin. Chem. Biol.* **2006**, *10*, 658–663
- (28) Carre-Burritt, A. E.; Van Hoomissen, D. J.; Vyas, S. Role of pH in the Transformation of Perfluoroalkyl Carboxylic Acids by Activated Persulfate: Implications from the Determination of Absolute Electron-Transfer Rates and Chemical Computations. *Environ. Sci. Technol.* **2021**, *55*, 8928–8936.
- (29) Wang, X. B.; Nicholas, J. B.; Wang, L. S. Photoelectron spectroscopy and theoretical calculations of SO4- and HSO4-: Confirmation of high electron affinities of SO4 and HSO4. *J. Phys. Chem. A* **2000**, *104*, 504–508.
- (30) Mckee, M. L. Computational Study of the Mono- and Dianions of SO₂, SO₃, SO₄, S₂O₃, S₂O₄, S₂O₆, and S₂O₈. *J. Phys. Chem.* **1996**, 100, 3473–3481.
- (31) Tang, Y.; Thorn, R. P.; Mauldin, R. L.; Wine, P. H. Kinetics and Spectroscopy of the SO₄⁻ Radical in Aqueous Solution. *Journal of Photochemistry and Photobiology, A: Chemistry* **1988**, 44, 243–258.
- (32) Méndez-Hernández, D. D.; Tarakeshwar, P.; Gust, D.; Moore, T. A.; Moore, A. L.; Mujica, V. Simple and accurate correlation of experimental redox potentials and DFT-calculated HOMO/LUMO energies of polycyclic aromatic hydrocarbons. *J. Mol. Model.* **2013**, *19*, 2845–2848.
- (33) Acelas, N.; Flórez, E.; Hadad, C.; Merino, G.; Restrepo, A. A Comprehensive Picture of the Structures, Energies, and Bonding in [SO4(H2O)n]2-, n = 1–6. *J. Phys. Chem. A* **2019**, *123*, 8650–8656.
- (34) Blades, A. T.; Kebarle, P. Study of the Stability and Hydration of Doubly Charged Ions in the Gas Phase: SO_4^{2-} , $S_2O_6^{2-}$, $S_2O_8^{2-}$, and Some Related Species. *J. Am. Chem. Soc.* **1994**, *116*, 10761–10766.
- (35) Smith, D. W. Ionic Hydration Enthalpies. *J. Chem. Educ.* **1977**, 54, 540–542.
- (36) Kelly, C. P.; Cramer, C. J.; Truhlar, D. G. SM6: A density functional theory continuum Solvation Model for calculating aqueous solvation free energies of neutrals, ions, and solute-water clusters. *J. Chem. Theory Comput.* **2005**, *1*, 1133–1152.

- (37) Bryantsev, V. S.; Diallo, M. S.; Goddard, W. A. Computational Study of Copper(II) Complexation and Hydrolysis in Aqueous Solutions Using Mixed Cluster/Continuum Models. *J. Phys. Chem. A* **2009**, *113*, 9559–9567.
- (38) Nadykto, A. B.; Yu, F.; Herb, J. Theoretical analysis of the gas-phase hydration of common atmospheric pre-nucleation (HSO₄⁻)-(H₂O)_n and (H₃O⁺)(H₂SO₄)(H₂O)_n cluster ions. *Chem. Phys.* **2009**, 360, 67–73.

□ Recommended by ACS

Dynamics of Ion Pairing in Dilute Aqueous HCl Solutions by Spectroscopic Measurements of Hydroxyl Radical Conversion into Dichloride Radical Anions

Lukasz Kazmierczak, Dorota Swiatla-Wojcik, et al.

AUGUST 12, 2021

THE JOURNAL OF PHYSICAL CHEMISTRY B

ABEEM/MM OH $^-$ Models for OH $^-$ (H $_2$ O) $_n$ Clusters and Aqueous OH $^-$: Structures, Charge Distributions, and Binding Energies

Hua Shi, Zhong-Zhi Yang, et al.

JUNE 10, 2020

THE JOURNAL OF PHYSICAL CHEMISTRY A

READ 🗹

 $\mathbf{S}_1\text{-State}$ Decay Dynamics of Benzenediols (Catechol, Resorcinol, and Hydroquinone) and Their 1:1 Water Clusters

Kuk Ki Kim, Sang Kyu Kim, et al.

AUGUST 25, 2021

THE JOURNAL OF PHYSICAL CHEMISTRY A

READ 🗹

Thermodynamic Properties: Enthalpy, Entropy, Heat Capacity, and Bond Energies of Fluorinated Carboxylic Acids

Suarwee Snitsiriwat, Joseph W. Bozzelli, et al.

JANUARY 03, 2022

THE JOURNAL OF PHYSICAL CHEMISTRY A

READ 🗹

Get More Suggestions >